Journal of Control, Automation and Electrical Systems (2020) 31:1–9
https://doi.org/10.1007/s40313-019-00552-0

Blood-Glucose Regulation Using Fractional-Order PID Control

Henrique Mohallem Paiva[1] · **Wagner Souza Keller**[1] · **Luísa Garcia Ribeiro da Cunha**[1]

Received: 20 January 2019 / Revised: 19 October 2019 / Accepted: 25 November 2019 / Published online: 9 December 2019

Abstract
This paper proposes a blood-glucose regulation approach employing a fractional-order proportional-integral-derivative (FOPID) controller, whose parameters are tuned using a numerical optimization methodology. The proposed technique is tested on 100 virtual patients using the Dalla Man model, an *in silico* type-1 diabetic patient model from the literature. The results are favorably compared with the ones obtained with a standard PID control. In a series of simulated tests, the FOPID approach leads to better results in terms of regulating the blood glucose levels between the specified limits, at the expense of requiring a higher, yet reasonable amount of insulin injected to the patient. Simulations were run for one day, and two different diets were considered. The quality of the regulation was measured in terms of the integral of blood glucose beyond the specified limits of 70 and 180 mg/dl. The values obtained with the PID controller were 17.5 ± 18.9 and 13.1 ± 16.8 min g/dl, while the FOPID controller leads to values of 7.3 ± 9.3 and 7.0 ± 8.0 min g/dl, respectively. On the other hand, the FOPID increased the request amount of insulin, from 1.9 ± 1.6 and 1.7 ± 1.5 nmol/kg to 3.0 ± 2.2 and 2.7 ± 2.0 nmol/kg (still within the expected daily range of 3–6 nmol/kg of insulin).

Keywords Automatic control · Fractional control · FOPID · Blood-glucose regulation

1 Introduction

Designing an automatic glucose controller for a diabetic patient is a classic bioengineering problem which has been studied for almost six decades, since the seminal work of Arnold (Kadish 1963). This problem has gained attention in the last years, and much effort has been made toward the design of an artificial pancreas, which is the long-desired goal of this research (Haidar 2016).

The reader is referred to the work of Cobelli et al. (2009) for a comprehensive review of the research in blood-glucose control until 2009, including a detailed description of the patient models and of the involved signals. A shorter literature survey, updated until 2013, has been published by Lunze et al. (2013).

✉ Henrique Mohallem Paiva
hmpaiva@unifesp.br

Wagner Souza Keller
wkeller@unifesp.br

Luísa Garcia Ribeiro da Cunha
ribeiro.luisa@unifesp.br

[1] UNIFESP - Universidade Federal de Sao Paulo (Federal University of Sao Paulo), Rua Talim, 330, Sao Jose dos Campos, SP 12231-280, Brazil

More recently, Boiroux et al. (2018) studied an overnight glucose control problem employing a model predictive control (MPC) approach. An internal model control approach, with both offline and online tuning, has been proposed by Bhattacharjee et al. (2018). Saleem et al. (2018) have studied the controllability and observability of the glucose–insulin–glucagon system. Linear Matrix Inequalities (LMI) were studied by Nath et al. (2019). Adaptive techniques have also been studied Ahmad et al. (2019), Nath et al. (2018), as well as sliding mode control algorithms (Ahmad et al. 2017).

This paper proposes a new approach employing a fractional-order proportional-integral-derivative (FOPID) controller (Dastjerdi et al. 2018; Lu et al. 2018). To the best of the authors' knowledge, this control methodology has never been applied to this problem.

The controller is used to define the amount of insulin to be injected to the patient, according to the blood glucose concentration levels. The main purpose is to keep the blood glucose between established limits, avoiding both hypo- and hyperglycemia. The FOPID results are compared with the ones obtained with a standard PID controller (Lunze et al. 2013) and with those of a MPC approach (Gondhalekar et al. 2018).

The FOPID is superior to the classical PID controller due to the number of adjustment parameters—not only the

three parameters related to the PID action, but also two more indicating the derivator and integrator orders, which are not necessarily integer. The FOPID approach is expected to present more flexibility and better adaptability to the plant dynamical properties. Furthermore, our previous studies have shown that fractional-order systems of low order are capable to represent dynamical behaviors similar or better than the ones of integer-order systems of high order. However, it should be noted that the design is also more challenging, as it requires more parameters to be adjusted (Kadu and Patil 2016; Podlubny 1994).

Tuning the parameters of a standard PID controller is a well-known control problem, for which there are well-established solutions available (Astrom and Hagglund 1995). However, the choice of FOPID parameters is still a matter of research. To solve this problem, rule-of-thumb (Dastjerdi et al. 2018) and analytical methodologies have been proposed. On the other hand, recent papers have used numerical optimization algorithms, which minimize cost functions to find the parameters which lead to the desired controller performance. This is the approach adopted by Ates and Yeroglu (2016), who employed a Tabu Search-based algorithm; by Bingul and Karahan (2018), who used particle swarm optimization and artificial bee colony optimization; by Lu et al. (2018), who adopted a quantum bacterial foraging algorithm; by Ramezanian et al. (2013), who also used particle swarm optimization; and by Verma et al. (2017), who employed a gray wolf optimizer. Similarly, a numerical approach is adopted in this paper, which uses the Nelder–Mead algorithm (Lagarias et al. 1998) to solve the optimization problem. In order to perform a fair comparison, the same methodology is used to tune the integer-order and fractional-order PID controllers.

Since the classic minimal model of Bergman (1989), several nonlinear physiological *in silico* models have been developed to simulate the glucose–insulin interaction in virtual patients (Colmegna et al. 2018; Hovorka et al. 2008; Kanderian et al. 2009; Mansell et al. 2017. In this paper, the Dalla Man model (Dalla Man et al. 2007a, b) was chosen to simulate type-1 diabetic subjects because it is more complete than other available models and represents credible real-life patients.

This text is organized as follows. Section 2 briefly reviews the adopted patient model. Section 3 describes the FOPID controller structure and the adopted tuning methodology. Section 4 presents the results. Finally, conclusions are discussed in Sect. 5.

2 Patient Model

As mentioned in the introduction, this paper adopts the Dalla Man model, whose subsystems are briefly described in this section. For each subsystem, a short description, the governing equations, the initial conditions and a table explaining the variables and parameters are presented .

This summarized model description is presented here to allow the reader to understand the main characteristics of the patient model adopted in this work. For a detailed model description and an in-depth discussion of each variable and parameter, please refer to the original works (Cobelli et al. 2009; Dalla Man et al. 2007a, b).

Table 1 Variables and parameters of the glucose subsystem (Dalla Man et al. 2007b)

G	Plasma glucose concentration (mg/dl)
G_p	Glucose mass in the plasma and in rapidly equilibrating tissues (mg/kg)
G_t	Glucose mass in slowly equilibrating tissues (mg/kg)
EGP	Endogenous glucose production (produced by the liver) (mg/kg/min)
R_a	Appearance rate of glucose in plasma (from the gastrointestinal tract subsystem) (mg/kg/min)
U_{ii}, U_{id}	Insulin-independent and insulin-dependent glucose utilization by the muscle and adipose tissue subsystem (mg/kg/min)
E	Renal excretion (from the kidney subsystem) (mg/kg/min)
V_G	Distribution volume of glucose (dl/kg)
k_1, k_2	Rate parameters (1/min)

2.1 Glucose Subsystem

This subsystem, which describes the glucose dynamics, is represented by the following set of equations (Dalla Man et al. 2007b), whose variables and parameters are described in Table 1.

In this and other subsystems, the suffix b used in the initial conditions stands for basal state.

$$\begin{aligned} G(t) &= \frac{G_p(t)}{V_G} \\ \dot{G}_p(t) &= EPG(t) + R_a(t) + U_{ii}(t) - \\ &\quad - E(t) - k_1 \cdot G_p(t) + k_2 \cdot G_t(t) \\ \dot{G}_t(t) &= -U_{id}(t) + k_1 \cdot G_p(t) - k_2 \cdot G_t(t) \\ G(0) &= G_b, \quad G_p(0) = G_{pb}, \quad G_t(0) = G_{tb} \end{aligned} \tag{1}$$

2.2 Insulin Subsystem

This subsystem, which describes the insulin dynamics, is represented by the following set of equations (Dalla Man et al. 2007a, b), whose variables and parameters are described in Table 2.

Table 2 Variables and parameters of the insulin subsystem (Dalla Man et al. 2007a, b)

I	Plasma insulin concentration (pmol/dl)
I_p	Insulin mass in the plasma (pmol/kg)
I_l	Insulin mass in the liver (pmol/kg)
R_i	Rate of insulin appearance in plasma (pmol/kg/min) (from the subcutaneous insulin infusion subsystem)
V_I	Distribution volume of insulin (l/kg)
m_1, m_2, m_3, m_4	Rate parameters (1/min)

Table 3 Variables and parameters of the gastrointestinal tract subsystem (Dalla Man et al. 2007b)

Q_sto	Total glucose mass in the stomach (mg)
Q_sto1	Glucose mass in the stomach (solid) (mg)
Q_sto2	Glucose mass in the stomach (liquid) (mg)
Q_gut	Glucose mass in the intestine (mg)
D	Mass of ingested glucose (mg)
$k_\mathrm{gri}, k_\mathrm{empt}, k_\mathrm{abs}$	Rate parameters (1/min)
f	Fraction of absorbed intestinal glucose which appears in plasma
BM	Body mass (kg)

$$
\begin{aligned}
I(t) &= \frac{I_\mathrm{p}(t)}{V_\mathrm{I}} \\
\dot{I}_\mathrm{p}(t) &= -(m_1 + m_3(t)) \cdot I_l(t) + m_2 \cdot I_\mathrm{p}(t) \\
\dot{I}_l(t) &= -(m_2 + m_4) \cdot I_\mathrm{p}(t) + m_1 \cdot I_l(t) + R_\mathrm{i}(t) \\
I(0) &= I_\mathrm{b}, \quad I_\mathrm{p}(0) = I_\mathrm{pb}, \quad I_l(0) = I_\mathrm{lb}
\end{aligned}
\tag{2}
$$

2.3 Gastrointestinal Tract Subsystem

This subsystem, which models the transportation of glucose through the stomach and intestine, is described by the following set of equations (Dalla Man et al. 2007b), whose variables and parameters are described in Table 3 (R_a is described in Table 1).

$$
\begin{aligned}
Q_\mathrm{sto}(t) &= Q_\mathrm{sto1}(t) + Q_\mathrm{sto2}(t) \\
\dot{Q}_\mathrm{sto1}(t) &= d \cdot D(t) - K_\mathrm{gri} \cdot Q_\mathrm{sto1}(t) \\
\dot{Q}_\mathrm{sto2}(t) &= k_\mathrm{gri} \cdot Q_\mathrm{sto1}(t) - k_\mathrm{empt}(Q_\mathrm{sto}) \cdot Q_\mathrm{sto2}(t) \\
\dot{Q}_\mathrm{gut}(t) &= k_\mathrm{empt}(Q_\mathrm{sto}) \cdot Q_\mathrm{sto2}(t) - k_\mathrm{abs} \cdot Q_\mathrm{gut}(t) \\
R_\mathrm{a}(t) &= \frac{f \cdot k_\mathrm{abs} \cdot Q_\mathrm{gut}(t)}{BM} \\
Q_\mathrm{sto1}(t) &= 0, \quad Q_\mathrm{sto2}(t) = 0, \quad Q_\mathrm{gut}(t) = 0
\end{aligned}
\tag{3}
$$

2.4 Liver Subsystem

This subsystem, which models the relevant dynamics in the liver, is described by the following set of equations (Dalla Man et al. 2007b), whose variables and parameters are described in Table 4 (EGP is described in Table 1).

Table 4 Variables and parameters of the liver subsystem (Dalla Man et al. 2007b)

I_po	Insulin in the portal vein (pmol/kg)
I_l	Intermediate signal to generate I_d
I_d	Delayed insulin signal (pmol/l)
k_p1	Extrapolated EGP at zero glucose and insulin (mg/kg/min)
k_p2	Liver glucose effectiveness (1/min)
$k_\mathrm{p3}, k_\mathrm{p4}$	Parameters which define insulin action
k_i	Rate parameter (1/min)

Table 5 Variables and parameters of the muscle and adipose tissue subsystem (Dalla Man et al. 2007b)

U	Total glucose utilization
U_ii	Insulin-independent utilization (constant)
U_id	Insulin-dependent utilization
V_m, K_m	Auxiliary variables, both linear functions of $X(t)$
X	Insulin in the interstitial fluid
I	Plasma insulin (from insulin subsystem)
p_{2u}	Constant representing insulin action (1/min)

$$
\begin{aligned}
\mathrm{EGP}(t) &= k_\mathrm{p1} - k_\mathrm{p2} \cdot G_\mathrm{p}(t) - k_\mathrm{p3} \cdot I_\mathrm{d}(t) \\
&\quad -k_\mathrm{p4} \cdot I_\mathrm{po}(t), \mathrm{EGP} \geq 0 \\
\dot{I}_1(t) &= -k_\mathrm{i} \cdot (I_1(t) - I(t)) \\
\dot{I}_\mathrm{d}(t) &= -k_\mathrm{i} \cdot (I_\mathrm{d}(t) - I_1(t)) \\
\mathrm{EGP}(0) &= \mathrm{EGP}_\mathrm{b}, \quad I_1(0) = I_\mathrm{b}, \quad I_\mathrm{d}(0) = I_\mathrm{b}
\end{aligned}
\tag{4}
$$

2.5 Muscle and Adipose Tissue Subsystem

The description of the muscle and body tissue (adipose tissue) in this model is related with glucose utilization. It is described by the following set of equations (Dalla Man et al. 2007b), whose variables and parameters are described in Table 5.

$$
\begin{aligned}
U(t) &= U_\mathrm{ii} + U_\mathrm{id}(t) \\
U_\mathrm{id}(t) &= V_m(X(t)) \cdot \frac{G_t(t)}{K_m(X(t)) + G_t(t)} \\
\dot{X}(t) &= -p_{2u} \cdot X(t) + p_{2u} \cdot (I(t) - I_\mathrm{b}) \\
X(t) &= 0
\end{aligned}
\tag{5}
$$

2.6 Kidney Subsystem

Renal excretion $E(t)$ is proportional to the value of the plasma glucose G_p that exceeds a certain threshold. It is rep-

Table 6 Variables and parameters of the subcutaneous insulin infusion subsystem (Dalla Man et al. 2007a)

I_{sc1}, I_{sc2}	Amount of nonmonomeric and monomeric insulin in the subcutaneous space
IIR	Exogenous insulin infusion rate (pmol/kg/min)
k_d, k_{a1}, k_{a2}	Rate constants (1/min)

resented by the following equation (Dalla Man et al. 2007b). Both variables are defined in Table 1.

$$E(t) = K_{e1} \cdot (G_p(t) - K_{e2}), \quad E(t) \geq 0 \tag{6}$$

2.7 Subcutaneous Insulin Infusion Subsystem

This subsystem describes the subcutaneous insulin infusion in a type-I diabetic patient. It is described by the following set of equations (Dalla Man et al. 2007a), whose variables and parameters are described in Table 6 (R_i is defined in Table 2).

$$\begin{aligned} \dot{I}_{sc1}(t) &= -(k_d + k_{ai}) \cdot I_{sc1}(t) + IIR(t) \\ \dot{I}_{sc2}(t) &= k_d \cdot I_{sc1}(t) - k_{a2} \cdot I_{sc2}(t) \\ \dot{R}_i(t) &= k_{a1} \cdot I_{sc1}(t) + k_{a2} \cdot I_{sc2}(t) \end{aligned} \tag{7}$$

3 FOPID Controller

3.1 Controller Structure

In the adopted control strategy, the control variable is the insulin infusion IIR [Eq. (7)] and the system output is the plasma glucose concentration G [Eq. (1)], which is measured by a sensor with a delay of 10 min. As is customary, the error signal is defined by the difference between the output and a specified target value.

The FOPID controller has the following structure in the Laplace domain:

$$\begin{aligned} C(s) &= K_p + K_i s^{-\lambda} + K_d s^{\mu} = \\ &= K_p \left(1 + \frac{1}{T_i} s^{-\lambda} + T_d s^{\mu}\right), \quad \lambda, \mu \geq 0 \end{aligned} \tag{8}$$

where K_p, K_i and K_d are the proportional, integral and derivative gains, T_i and T_d are time constants, and λ and μ are the fractional integral and derivative orders, respectively. A standard PID controller has $\lambda = \mu = 1$. Due to these two additional parameters, the FOPID controller can be more complex to be designed but also more accurate and flexible that the PID controller.

In the time domain, the relationship between the error signal $e(t)$ and the control variable $u(t)$ can be expressed as Podlubny (1994):

$$u(t) = K_p e(t) + K_i D^{-\lambda} e(t) + K_d D^{\mu} e(t) \tag{9}$$

The definition of the integro-differential operator ${}_a D_t^q$ (which can be used not only for integer-order equations, but also for non-integer ones) is given by Eq. (10) (Dalau et al. 2017).

$${}_a D_t^q = \begin{cases} \dfrac{d^q}{dt^q}, & q > 0 \\ 1, & q = 0 \\ \int_a^t (d\tau)^{-q}, & q < 0 \end{cases} \tag{10}$$

This is a generalization of the integral and differential operators, where q is the order of the derivative and can be a real or a complex number, and a is a constant related to the initial conditions.

There are several definitions for fractional integral and derivatives. The Caputo definition is given in Eq. (11) (Dalau et al. 2017; Podlubny 1994):

$${}_a D_t^q f(t) = \begin{cases} \dfrac{d^m f(t)}{dt^m}, & q = m \in \mathbb{N} \\ \dfrac{1}{\Gamma(m-q)} \displaystyle\int_0^t \frac{f^{(m)}\tau}{(t-\tau)^{q+1-m}} d\tau, & m = \lfloor q \rfloor \end{cases} \tag{11}$$

where $\Gamma(x) = \int_0^\infty t^{x-1} e^{-t} dt$ is known as the Gamma Function. Taking the Laplace transform of the Caputo derivative, the result is given in Eq. (12) (Dalau et al. 2017):

$$\mathcal{L}\{{}_0 D_t^q f(t)\} = s^\alpha F(s) - \sum_{k=0}^{m-1} s^{\alpha-1-k} f^{(k)}(t)|_{t=0} \tag{12}$$

Assuming null initial conditions, Eq. (12) can be simplified by $s^\alpha F(s)$ (Dalau et al. 2017).

Since the fractional-order integro-differential equations usually do not have an analytical solution, it is necessary to use a numerical approximation to find one. In this paper, the CRONE methodology (Lanusse et al. 2015) has been used to implement the fractional terms of the controller (CRONE, *Commande Robuste d'Ordre Non Entier*, is the French acronym for robust fractional-order control).

This approach is based on a closed-loop system, which can be implemented in a open-loop system using a fractional-order integrator and differentiator.

Suppose we have $P(s) = s^\alpha$, with $\alpha > 0$ and non-integer, and we want to find an approximation for $P(s)$. That can be accomplished using the CRONE methodology. We can assume that $P(s)$ is equal (or at least approximate) to a transfer function of a Nth-order filter which has the same number of poles and zeros in a frequency range $[\omega_l, \omega_h]$ This is shown in the second-order section (SOS), Eq. (13) (Dalau et al. 2017; Valerio and Sa da Consta 2013).

$$s^{\alpha} = C \prod_{m=1}^{N} \frac{1 + \frac{s}{\omega_{z,m}}}{1 + \frac{s}{\omega_{\mathrm{p,m}}}} \tag{13}$$

with C being the gain of this system and $\omega_{p,m}$ and $\omega_{z,m}$ being the poles and zeros, respectively. The poles and zeros are described by Eqs. 14 and 15 (Valerio and Sa da Consta 2013):

$$\omega_{z,m} = w_{\mathrm{i}} \left(\frac{w_h}{w_{\mathrm{i}}} \right)^{\frac{2m-1-\alpha}{2N}} \tag{14}$$

$$\omega_{\mathrm{p,m}} = w_{\mathrm{i}} \left(\frac{w_h}{w_{\mathrm{i}}} \right)^{\frac{2m-1+\alpha}{2N}} \tag{15}$$

The order of the transfer function in Eq. (13) should be chosen so that the error is minimal. For a perfect approximation, the order should be infinite. However, we can stipulate the minimal error to be less than some value E, to do so we set the order N of the filter used in the approximation as described in Eq. (16).

$$N = \left\lceil \frac{\log\left(\frac{\omega_h}{\omega_l}\right)}{\frac{E}{10}\left(\frac{1}{1+q} + \frac{1}{2-q}\right)} \right\rceil \tag{16}$$

Although this example has been all about a fractional-order differentiator, the same approximation can be used for a fractional-order integrator.

3.2 Parameter Tuning

The controller parameter tuning was performed using the Nelder–Mead algorithm (Lagarias et al. 1998), which was used to find the parameter set which minimizes a given cost function J. The defined cost function is composed by two additive terms: J_{e}, to penalize the output error, and J_u, to penalize the control effort.

A target is set at a plasma glucose of 125 mg/dl, and a tolerance of ± 55 mg/dl is established. Therefore, the minimum and maximum blood glucose concentrations are, respectively:

$$\begin{aligned} G_{\min} &= 70 \text{ mg/dl} \\ G_{\max} &= 180 \text{ mg/dl} \end{aligned} \tag{17}$$

The following metric $G_{\mathrm{err}}(t)$ is defined to quantify, in mg/dl, the amount of blood glucose beyond the specified limits at a given instant t:

$$\begin{aligned} G_{\mathrm{err}}(t) &= G_{\mathrm{blw}}(t) + G_{\mathrm{abv}}(t) \\ G_{\mathrm{blw}}(t) &= \min(G_{\min} - G(t), 0) \\ G_{\mathrm{abv}}(t) &= \min(G(t) - G_{\max}, 0) \end{aligned} \tag{18}$$

where $\min(a, b)$ represents the minimum between the real variables a and b.

For a simulated experiment with a duration of t_{f} minutes, the following cost function J_{e} is defined to quantify the total amount of blood glucose beyond the specified limits:

$$J_{\mathrm{e}} = \int_0^{t_{\mathrm{f}}} G_{\mathrm{err}}(t)\mathrm{d}t \tag{19}$$

The expression of J_{e} is similar to the standard IAE (integral of the absolute error) metric. The difference is that a tolerance around the setpoint was adopted.

Similarly, the following cost function J_u is defined to quantify the control effort, measured in terms of insulin infusion:

$$J_u = \int_0^{t_{\mathrm{f}}} IIR(t)\mathrm{d}t \tag{20}$$

The overall cost function to be minimized is given by:

$$J = 100 J_{\mathrm{e}} + J_u \tag{21}$$

where the factor of 100 was chosen to weigh the cost function. It means that an eventual transgression in the glucose concentration, represented by the cost J_{e}, is more penalized than the control effort represented by J_u.

In spite of being less penalized, it should be noted that J_u is not negligible, that is, it shall not be removed from Eq. (21). Otherwise, the probable result would be a controller which would require an unreasonable amount of insulin to regulate the blood glucose, which would not be feasible in practice.

4 Results and Discussion

The controller parameters were tuned by using the methodology described in Sect. 3, and the obtained values are presented in Table 7.

It is particularly noteworthy the integrative order λ of the FOPID controller, which is five orders of magnitude lower than 1, indicating that the obtained fractional integrator behaves almost as an additional proportional term. This result means that the adopted optimization approach lead to a FOPID controller with essentially no integral action, only proportional and derivative ones. Such outcome could be ascribed to the tolerance of ± 55 mg/dl established around the setpoint; with such tolerance, a zero steady-state error would not be required, and therefore the integral action would arguably not be necessary.

Simulations were run for 100 different virtual adult patients during a day. In order to reproduce real scenarios, two diets were adopted:

Table 7 PID and FOPID controller parameters

Parameter	PID	FOPID	unit
K_p	9.034e−04	2.756e−03	pmol/kg/min per mg/dl
T_d	1.227e+02	1.539e+02	$(\text{min})^{\mu}$
T_i	1.699e−01	2.292e−01	$(\text{min})^{\lambda}$
μ	1	2.883e−01	–
λ	1	3.165e−05	–

– Each patient following diet 1 was fed three meals containing 45 g, 70 g and 70 g of glucose, at 8, 12 and 20 h, respectively.

– Each patient following diet 2 was fed three meals containing 60 g of glucose each, at 8, 13 and 21 h.

The main simulation results, for both controllers and both diets, are presented in Figs. 1, 2, 3 and 4. The results are then summarized in Table 8.

A visual analysis of Figs. 1a and 3a indicates that the PID controller, on average, already presents a good blood-glucose regulation. This result was expected, for the PID controller has been widely used in this context and its advantages are known (Cobelli et al. 2009; Lunze et al. 2013). However, these figures also show that there is room for improvement,

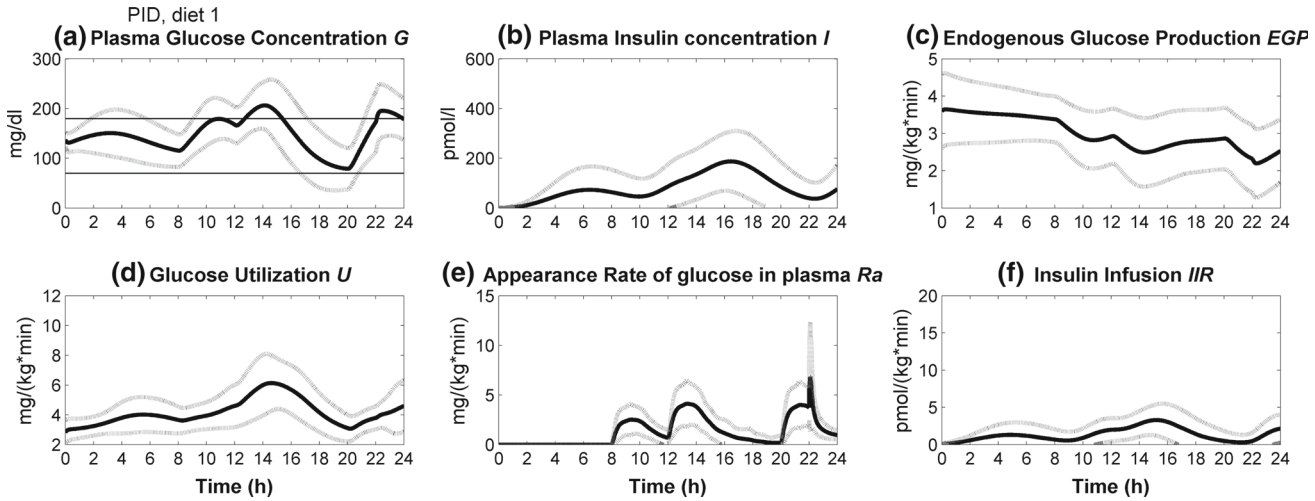

Fig. 1 Simulation results using the PID controller during one day, considering diet 1. The thick black line indicates the mean value for 100 different virtual patients. The dashed gray lines indicates the mean value plus and minus one standard deviation. The horizontal lines in **a** indicate the established limits of 70 and 180 mg/dl

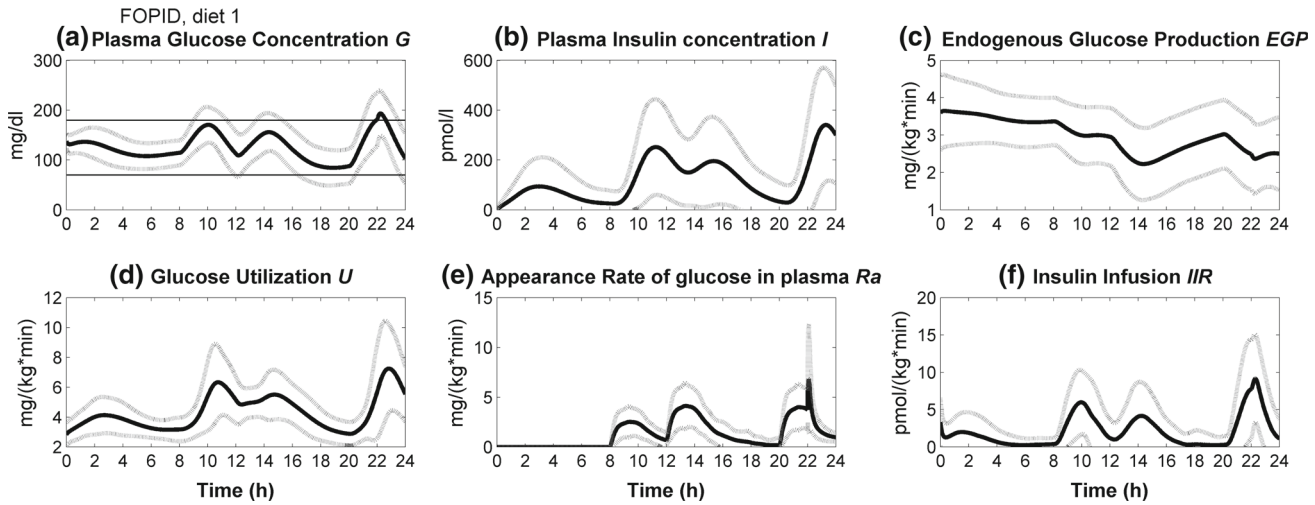

Fig. 2 Simulation results using the FOPID controller during one day, considering diet 1. The thick black line indicates the mean value for 100 different virtual patients. The dashed gray lines indicate the mean value plus and minus one standard deviation. The horizontal lines in **a** indicate the established limits of 70 and 180 mg/dl

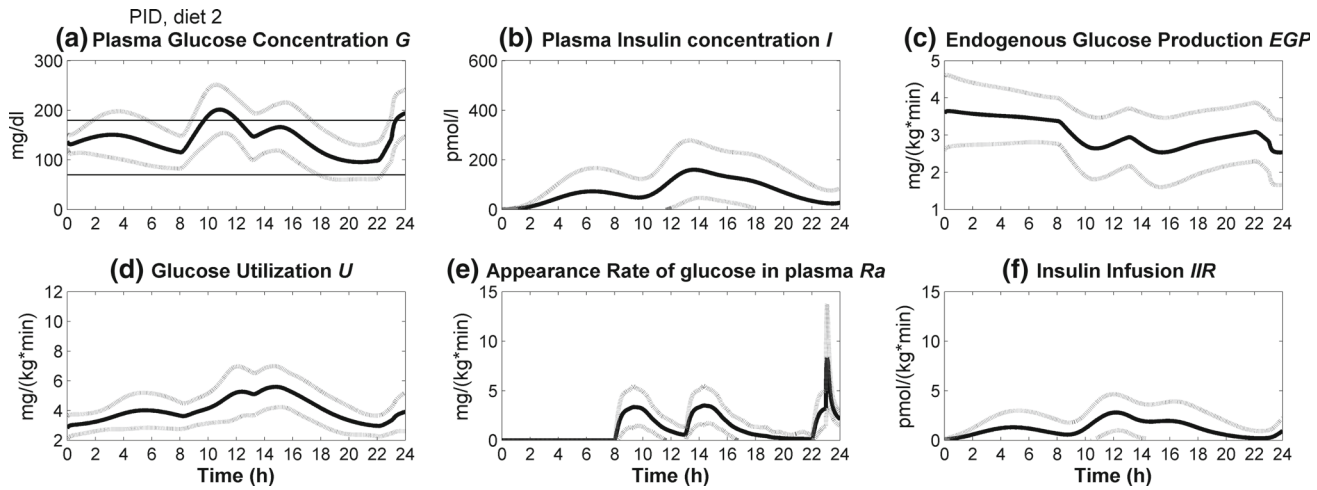

Fig. 3 Simulation results using the PID controller during one day, considering diet 2. The thick black line indicates the mean value for 100 different virtual patients. The dashed gray lines indicates the mean value plus and minus one standard deviation. The horizontal lines in **a** indicate the established limits of 70 and 180 mg/dl

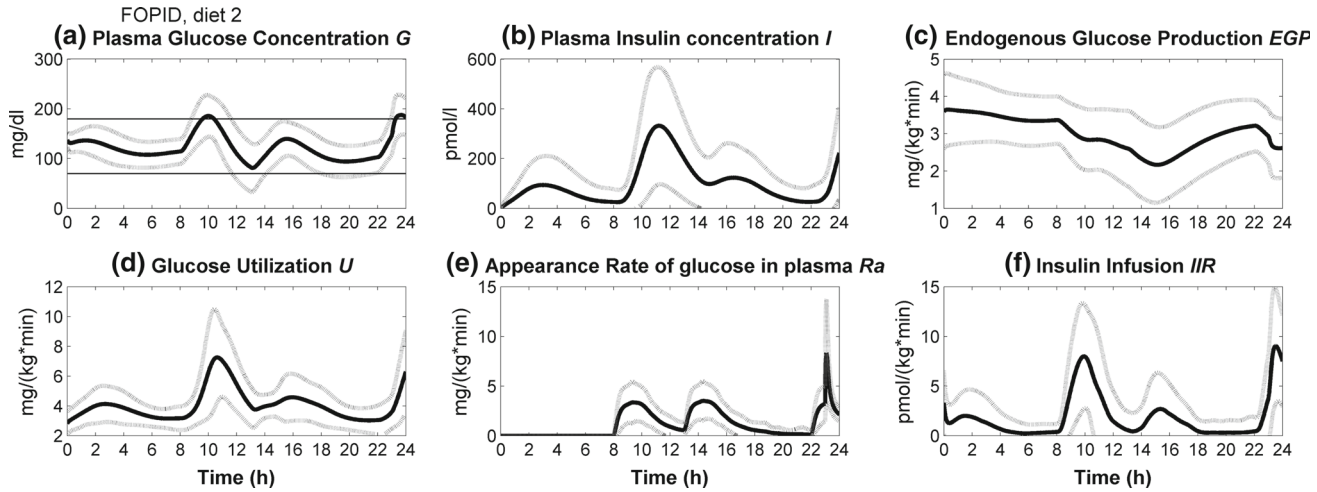

Fig. 4 Simulation results using the FOPID controller during one day, considering diet 2. The thick black line indicates the mean value for 100 different virtual patients. The dashed gray lines indicate the mean value plus and minus one standard deviation. The horizontal lines in **a** indicate the established limits of 70 and 180 mg/dl

Table 8 Summary of the results during a day, considering all 100 virtual patients (mean ± standard deviation)

	PID	FOPID	Unit
(a) Integral of the blood glucose beyond the specified limits [Eq. (19)]			
Diet 1	17.5 ± 18.9	7.3 ± 9.3	min × g/dl
Diet 2	13.1 ± 16.8	7.0 ± 8.0	min × g/dl
(b) Total amount of injected insulin [Eq. (20)]			
Diet 1	1.9 ± 1.6	3.0 ± 2.2	nmol/kg
Diet 2	1.7 ± 1.5	2.7 ± 2.0	nmol/kg

for there are violations (although not severe) of the desired blood glucose limits. In fact, Figs. 2a and 4a show that the FOPID controller is able to keep better the blood glucose inside the specified limits.

The qualitative analysis presented in the previous paragraph can be quantified by the integral along time of the blood glucose values beyond the specified limits of 70 and 180 mg/dl. This value is presented in Table 8(a), which shows, for both diets, a better mean result (smaller violations) when the FOPID controller is used. It can be seen that the FOPID controller reduces the cost quantified in Table 8(a) by 58% (diet 1) and by 47% (diet 2)

A visual comparison between Figs. 1f, 2f, 3f and 4f shows that the FOPID controller requires a higher amount of injected insulin along time. However, the amount of required insulin at a given time is still acceptable, that is, no extremely high peak was observed. The total amount of injected insulin during a day is summarized in Table 8(b). This table indicates that the FOPID controller indeed required more insulin injected in a day than the PID controller. This increase, which is reasonable (i.e., not excessive), may be seen as the cost required by a better glucose regulation.

In fact, Hirsch (1999) states that the typical dosage of insulin for a patient with type 1 diabetes lies between 0.5 and 1.0 unit per kg per day, while Qu (2018) states that most insulin analogs have a formulation of 6 nmol per unit. Therefore, the typical daily dosage of insulin would lie between 3 and 6 nmol/kg. Hence, the daily values of 3.0 ± 2.2 nmol/kg and 2.7 ± 2.0 nmol/kg calculated by the controller proposed here are within the expected range.

The figures show that, for the FOPID control, the peak of insulin injection IIR (the control variable) does not exceed 20 pmol/(kg x min). This value is much lower than the ones that can be achieved by commercial insulin pumps. For instance, Regittnig et al. (2019) compared two pump models. The slowest one is able to deliver at most 0.025 units of insulin per second; for a patient with 100 kg, this rate is equivalent to 90 pmol/(kg min). The fastest one, on the other hand, can deliver insulin at a rate of 0.5 units/s, that is, 1800 pmol/(kg min), considering again an 100-kg patient. Therefore, the control effort required by the proposed controller is far from reaching the actuation limits.

The plasma insulin concentration, indicated in Figs. 1, 2, 3 and 4b, is higher for the FOPID controller, which is a natural consequence of the higher amount of insulin being injected to the patient. It is interesting to note that peaks in insulin injection (subfigures (f)) are usually followed by peaks in glucose utilization (subfigures (d)). The other two representative variables depicted in the figures, namely (c) endogenous glucose production and (e) appearance rate of glucose in plasma, present a similar behavior (considering the same diet), regardless of the use of a PID or a FOPID controller.

Gondhalekar et al. (2018) have proposed an improved model predictive control approach for blood-glucose control and have also used the Dalla Man model. Their simulation results for unannounced meals (as in our case) are presented in Figure 4 of Gondhalekar et al. (2018), left side. A comparison of this figure with our Figs. 2a and 4a shows that our FOPID approach leads to similar blood-glucose regulation results. The FOPID has the advantage of having a simpler implementation than the MPC. On the other hand, the MPC presents *a priori* guarantees that lack in the FOPID approach. This drawback in our approach can be overcome in future works by combining both methodologies, i.e., by including fractional calculus in the MPC technique.

A limitation of the present study was the use of simulated patients only. As the research progresses, clinical trials would be required, such as the ones described in Gondhalekar et al. (2018).

5 Conclusions

This paper proposed a new blood-glucose regulation methodology employing a fractional-order proportional-integral-derivative (FOPID) controller. The main contribution is the use of the fractional-order approach in this context.

The results were validated using a highly nonlinear and fairly complete *in silico* patient model, proposed earlier by Dalla Man and associates.

The obtained FOPID controller presented relevant proportional and derivative actions and negligible integral action.

A comparison between the results of a FOPID controller and of a standard PID controller was presented. Better regulation results were obtained with the FOPID controller. This outcome was to be expected because the PID approach can be seen as a particular instance of the FOPID methodology, where the orders of the integrator and derivator are constrained to be 1. Therefore, if the same technique is adopted to tune the parameters of both controllers, the one with a more general structure is expected to lead to better results.

The FOPID controller leads to a smaller output error, but also required a higher amount of insulin. This result can be ascribed to the way cost function J was defined [Eq. (21)], which penalized the output error significantly more than the control effort.

Future works could exploit other techniques to tune the FOPID controller parameters (Dastjerdi et al. 2018; Lu et al. 2018; Ramezanian et al. 2013; Verma et al. 2017). Furthermore, adaptive (Biswas et al. 2018) and robust (Zhang et al. 2019) FOPID approaches could be studied in the context of blood-glucose regulation.

Acknowledgements The authors are indebted to Prof. Claudio Cobelli (University of Padova, Italy) for sharing part of the computational code that was used in this work. Furthermore, the authors gratefully acknowledge the suggestions of Prof. Karina Rabello Casali (Federal University of Sao Paulo, UNIFESP, Brazil) and Prof. Karl Heinz Kienitz (Aeronautical Institute of Technology, ITA, Brazil). Finally, the contributions of Mr. Ayrton Casella (UNIFESP) in the first draft of this manuscript are also gratefully acknowledged.

References

Ahmad, S., Ahmed, N., Ilyas, M., & Khan, W. (2017). Super twisting sliding mode control algorithm for developing artificial pancreas

in type 1 diabetes patients. *Biomedical Signal Processing and Control*, *38*, 200–211.

Ahmad, I., Munir, F., & Munir, M. F. (2019). An adaptive backstepping based non-linear controller for artificial pancreas in type 1 diabetes patients. *Biomedical Signal Processing and Control*, *47*, 49–56.

Astrom, K. J., & Hagglund, T. (1995). *PID controllers: Theory, design, and tuning*. Research Triangle Park, NC: Instrument society of America.

Ates, A., & Yeroglu, C. (2016). Optimal fractional order PID design via Tabu search based algorithm. *ISA Transactions*, *60*, 109–118.

Bergman, R. N. (1989). Toward physiological understanding of glucose tolerance: Minimal-model approach. *Diabetes*, *38*(12), 1512–1527.

Bhattacharjee, A., Easwaran, A., Leow, M. K. S., & Cho, N. (2018). Evaluation of an artificial pancreas in in silico patients with online-tuned internal model control. *Biomedical Signal Processing and Control*, *41*, 198–209.

Bingul, Z., & Karahan, O. (2018). Comparison of PID and FOPID controllers tuned by PSO and ABC algorithms for unstable and integrating systems with time delay. *Optimal Control Applications and Methods*, *39*(4), 1431–1450.

Biswas, D., Sharma, K. D., & Sarkar, G. (2018). Stable adaptive NSOF domain FOPID controller for a class of non-linear systems. *IET Control Theory & Applications*, *12*(10), 1402–1413.

Boiroux, D., Duun-Henriksen, A. K., Schmidt, S., Nørgaard, K., Madsbad, S., & Poulsen, N. K. (2018). Overnight glucose control in people with type 1 diabetes. *Biomedical Signal Processing and Control*, *39*, 503–512.

Cobelli, C., Dalla Man, C., Sparacino, G., Magni, L., De Nicolao, G., & Kovatchev, B. P. (2009). Diabetes: Models, signals, and control. *IEEE Reviews in Biomedical Engineering*, *2*, 54–96.

Colmegna, P., Sanchez-Pena, R. S., & Gondhalekar, R. (2018). Linear parameter-varying model to design control laws for an artificial pancreas. *Biomedical Signal Processing and Control*, *40*, 204–213.

Dalau, M., Gligor, A., & Dalau, T. M. (2017). Fractional order controllers versus integer order controllers. *Procedia Engineering*, *181*, 538–545.

Dalla Man, C., Raimondo, D. M., Rizza, R. A., & Cobelli, C. (2007a). GIM, simulation software of meal glucose–Insulin model. *Journal of Diabetes Science and Technology*, *1*(3), 323–330.

Dalla Man, C., Rizza, R. A., & Cobelli, C. (2007b). Meal simulation model of the glucose–insulin system. *IEEE Transactions on Biomedical Engineering*, *54*(10), 1740–1749.

Dastjerdi, A. A., Saikumar, N., & HosseinNia, H. (2018). Tuning guidelines for fractional order PID controllers: Rules of thumb. *Mechatronics*, *56*, 26–36.

Gondhalekar, R., Dassau, E., & Doyle, F. J., III. (2018). Velocity-weighting and velocity-penalty MPC of an artificial pancreas: Improved safety and performance. *Automatica*, *91*, 105–117.

Haidar, A. (2016). The artificial pancreas: How closed-loop control is revolutionizing diabetes. *IEEE Control Systems*, *36*(5), 28–47.

Hirsch, I. B. (1999). Type 1 diabetes mellitus and the use of flexible insulin regimens. *American Family Physician*, *60*(8), 2343–52.

Hovorka, R., Chassin, L. J., Ellmerer, M., Plank, J., & Wilinska, M. E. (2008). A simulation model of glucose regulation in the critically ill. *Physiological Measurement*, *29*(8), 959.

Kadish, A. H. (1963). Automation control of blood sugar a servomechanism for glucose monitoring and control. *ASAIO Journal*, *9*(1), 363–367.

Kadu, C. B., & Patil, C. Y. (2016). Design and implementation of stable PID controller for interacting level control system. *Procedia Computer Science*, *79*, 737–746.

Kanderian, S. S., Weinzimer, S., Voskanyan, G., & Steil, G. M. (2009). Identification of intraday metabolic profiles during closed-loop glucose control in individuals with type 1 diabetes. *Journal of Diabetes Science and Technology*, *3*(5), 1047–1057.

Lagarias, J. C., Reeds, J. A., Wright, M. H., & Wright, P. E. (1998). Convergence properties of the Nelder–Mead simplex method in low dimensions. *SIAM Journal on Optimization*, *9*(1), 112–147.

Lanusse, P., Sabatier, J., & Oustaloup, A. (2015). *Fractional order PID and first generation CRONE control system design. Fractional order differentiation and robust control design* (pp. 63–105). Dordrecht: Springer.

Lu, L. I. U., Liang, S. H. A. N., Yuewei, D. A. I., Chenglin, L. I. U., & Zhidong, Q. I. (2018). Improved quantum bacterial foraging algorithm for tuning parameters of fractional-order PID controller. *Journal of Systems Engineering and Electronics*, *29*(1), 166–175.

Lunze, K., Singh, T., Walter, M., Brendel, M. D., & Leonhardt, S. (2013). Blood glucose control algorithms for type 1 diabetic patients: A methodological review. *Biomedical Signal Processing and Control*, *8*(2), 107–119.

Mansell, E. J., Docherty, P. D., & Chase, J. G. (2017). Shedding light on grey noise in diabetes modelling. *Biomedical Signal Processing and Control*, *31*, 16–30.

Nath, A., Deb, D., Dey, R., & Das, S. (2018). Blood glucose regulation in type 1 diabetic patients: An adaptive parametric compensation control-based approach. *IET Systems Biology*, *12*(5), 219–225.

Nath, A., Dey, R., & Aguilar-Avelar, C. (2019). Observer based nonlinear control design for glucose regulation in type 1 diabetic patients: An LMI approach. *Biomedical Signal Processing and Control*, *47*, 7–15.

Podlubny, I. (1994). *Fractional-order systems and fractional-order controllers*. Bratislava: Institute of Experimental Physics, Slovak Academy of Sciences.

Qu, Y., et al. (2018). Dose unit establishment for a new basal insulin using joint modeling of insulin dose and glycemic response. *Journal of Diabetes Science and Technology*, *12*(1), 155–162.

Ramezanian, H., Balochian, S., & Zare, A. (2013). Design of optimal fractional-order PID controllers using particle swarm optimization algorithm for automatic voltage regulator (AVR) system. *Journal of Control, Automation and Electrical Systems*, *24*(5), 601–611.

Regittnig, W., Urschitz, M., Lehki, B., Wolf, M., Kojzar, H., Mader, J. K., et al. (2019). Insulin bolus administration in insulin pump therapy: Effect of bolus delivery speed on insulin absorption from subcutaneous tissue. *Diabetes Technology and Therapeutics*, *21*(1), 44–50.

Saleem, M. U., Farman, M., Rizwan, M., & Ahmad, M. O. (2018). Controllability and observability of glucose insulin glucagon system in humans. *Chinese Journal of Physics*, *56*(5), 1909–1916.

Valerio, D., & Sa da Consta, J. (2013). An introduction to fractional control. *The Institution of Engineering and Technology, IET Control Engineering Series*, *91*, 121–124.

Verma, S. K., Yadav, S., & Nagar, S. K. (2017). Optimization of fractional order PID controller using grey wolf optimizer. *Journal of Control, Automation and Electrical Systems*, *28*(3), 314–322.

Zhang, S., Liu, L., & Cui, X. (2019). Robust FOPID controller design for fractional-order delay systems using positive stability region analysis. *International Journal of Robust and Nonlinear Control*, *29*(15), 5195–5212.